Advances and Applications in Mathematical Sciences
Volume 19, Issue 9, July 2020, Pages 873-888

ON CHARACTERSTIC OF AMPLITUDE RATIOS OF REFLECTED AND REFRACTED WAVES

NEELAM KUMARI[1], R. K. POONIA[2], PAWAN KUMAR[1,*] and VINOD KALIRAMAN[1]

Department of Mathematics
Chaudhary Devi Lal University
Sirsa 125055, Haryana, India
E-mail: neelamkumaricdlu@gmail.com
vsisaiya@gmail.com

Department of Mathematics
Chandigarh University
Mohali (Punjab) India-140413
Email: dr.rkpoonia@gmail.com

Abstract

In this problem to analysis more characteristic of amplitude ratios of various reflected and refracted wave at the interface between non-local micropolar elastic solid and fluid saturated porous solid. So, the wave propagates in the medium non-local micropolar solid and fluid saturated porous solid and separated by the interfaces $z = 0$ is studied. Longitudinal wave and coupled wave impinges obliquely on the interfaces. Amplitude ratios of different reflected and refracted waves have been computed numerically for this specific model and results obtained are revealed graphically with incidence angle.

1. Introduction

The micropolar theory of elasticity constructed by Eringen and his co-workers intended to be applied on such materials and for problems where the ordinary theory of elasticity fails because of microstructure in the materials. Micropolar elastic materials, roughly speaking, are the classical elastic materials with extra independent degree of freedom for the local rotations.

2010 Mathematics Subject Classification: 37N10, 37N15, 74B10, 74L05, 76S05.
Keywords: reflected, refracted, non-local micropolar elastic, fluid saturated porous, amplitude ratio.
*Corresponding author; E-mail: pawan7585@gmail.com
Received December 20, 2019; Accepted January 25, 2020

These materials respond to spin inertia, body and surface couples and as a consequence they exhibit certain new static and dynamic effects, e.g. new types of waves and couples stresses.

Eringen developed the theories of ‘micropolar continua’ and ‘microstructures continua’ which are special cases of the theory of ‘micromorphic continua’ earlier developed by Eringen and his coworkers [7]. Thus, the Eringen’s ‘3M’ theories (Micromorphic, Microstretch, Micropolar) are the generalization the classical theory of elasticity. In classical continuum, each particle of a continuum is represented by a geometrical point and can have three degree of freedom of translation during the process of deformations.

Eringen and Edelen [2] developed the nonlocal elasticity theories characterized by the presence of nonlocality residuals of fields. In nonlocal theory of elasticity, the stress at any reference point within a continuous body depends not only on the strain at that point but also significantly influenced by the strains at all other points of the continuous body. Thus, the nonlocal stress forces act as a remote action forces. These types of forces are frequently encountered in atomic theory of lattice dynamics. The characteristic features of nonlocal theory may fall in the materials with microstructures, where the internal characteristic length may be considered as comparable with external characteristic length. There are so many authors related to waves and vibrations have been discussed. The present paper is concerned with waves propagate non-local micropolar elastic solid and fluid saturated porous solid. Find the values of amplitude ratios and with the help of MATLAB Software depicted in the graphs.

2. Basic Equations and Constitutive Relations

The basic equations for the reflection and refraction of inclination waves at the boundary of media M_1 and M_2 are discussed as

$$(1-\varepsilon^2\nabla^2)\sigma_{kl} = \lambda\delta_{kl}e_{rr}(x) + (\mu + K)e_{kl}(x) + \mu_{e_{lk}}(x) \tag{1}$$

$$(1-\varepsilon^2\nabla^2)\mu_{kl} = \alpha\lambda\delta_{kl}\gamma_{rr}(x) + \beta\gamma_{kl}(x) + \gamma\gamma_{lk}(x), \tag{2}$$

where σ_{kl} and μ_{kl} are using for the stresses; α, β, γ, K are representing the micrpolar elastic constants; λ, are Lame’s constants; $e_{kl} = (u_{kl} - \varepsilon_{klm}\phi_m)$ are relative distortion tensor u_i and ϕ_i are components of displacement and microrataion vector; $\gamma_{kl} = (\phi_{kl})$ are curvature tensor; $\varepsilon = (e_0 a)$ is the non-local parameter; e_0 and a are material constant and internal characteristic length respective and others symbols are their usual meaning.

The following equations of motion without body force and couple densities are given as

$$(\mu + \lambda)u_{k,kl} + (\mu + K)u_{l,kk} + K\varepsilon_{klm}\phi_{k,m} = \rho(1 - \varepsilon^2\nabla^2)\ddot{u}_1$$

$$(\alpha + \beta)\phi_{k,kl} + \gamma\phi_{1,kk} + K\varepsilon_{kmm}u_{n,m} - 2K\phi_1 = \rho j(1 - \varepsilon^2\nabla^2)\ddot{\phi}_1.$$

Now, using the Helmholtz decomposition

$$\{u, \phi\} = \nabla\{q, \xi\} + \nabla \times (U, \Pi), \nabla \cdot (U, \Pi) = 0.$$

Using above equation in (3) and (4) and assuming the wave form of potentials $\{q, \xi, U, \Pi\} = \{a, b, A, B\}\exp\{ik(\vec{n}\cdot\vec{r} - Vt\}$, propagating in the direction of unit vector $\vec{n}$ with the speed V. Therefore, four waves there exist in non-local isotropic micropolar elastic solid; such waves are independently longitudinal displacement wave, independently longitudinal micro-rotational wave and two sets of coupled transverse waves having their respective speed V_1, V_2, V_3 and V_4.

$$V_1^2 = c_1^2 + c_3^2 - \varepsilon^2\omega^2 \quad V_2^2 = \left(1 - \frac{2\omega_0^2}{\omega^2}\right)^{-1}(c_4^2 + c_5^2 - \varepsilon^2\omega^2) \tag{5}$$

$$V_3^2 = \frac{1}{2A}(-B + \sqrt{B^2 - 4AC}) \quad V_4^2 = \frac{1}{2A}(-B - \sqrt{B^2 - 4AC}), \tag{6}$$

where

$$A = 1 - \frac{2\omega_0^2}{\omega^2} \quad B = \varepsilon^2\omega^2 - c_4^2 - \frac{c_3^2\omega_0^2}{\omega^2} + A(\varepsilon^2\omega^2 - c_2^2 - c_3^2)$$

$$C = (\varepsilon^2\omega^2 - c_2^2 - c_3^2)(\varepsilon^2\omega^2 - c_4^2)$$

$$c_1^2 = \frac{\lambda + 2\mu}{\rho} \quad c_2^2 = \frac{\mu}{\rho} \quad c_3^2 = \frac{\kappa}{\rho}$$

$$c_4^2 = \frac{\gamma}{\rho j} \quad \omega_0^2 = \frac{\kappa}{\rho j}.$$

Every set of coupled transverse waves consists of a transverse displacement wave coupled with a transverse micro-rotational wave.

Assuming the 2-D problem by taking the following components of displacement and microrotation as

$$u = (u_1, 0, u_3) \quad \phi = (0, \phi_2, 0) \quad \frac{\partial}{\partial y} \equiv 0,$$

where

$$u_1 = q_x - U_{2,z} \quad u_3 = q_z + U_{2,x}$$

and components of stresses are

$$\sigma_{zz} = (\lambda + 2\mu + \kappa)\frac{\partial^2 q}{\partial z^2} + \lambda\frac{\partial^2 q}{\partial x^2} + (2\mu + \kappa)\frac{\partial^2 U_2}{\partial x \partial z}$$

$$\sigma_{zx} = (2\mu + \kappa)\frac{\partial^2 q}{\partial x \partial z} - (\mu + \kappa)\frac{\partial^2 U_2}{\partial z^2} + \mu\frac{\partial^2 U_2}{\partial x^2} - \kappa\phi_2$$

$$\mu_{zy} = \gamma\frac{\partial \phi_2}{\partial z}.$$

For medium M_2 (Fluid Saturated Porous Solid)

Using de Boer and Ehlers (1990), governing equations for deformation of an incompressible porous medium drenched with non-viscous fluid in non-existence of body forces are as follow

$$\nabla \cdot (\eta^S \dot{u}_S + \eta^F \dot{u}_F) = 0 \tag{10}$$

$$(\lambda^S + \mu^S)\nabla(\nabla \cdot u_S) + \mu^S \nabla^2 - \eta^S \nabla p - \rho^S \ddot{u}_s + S_v(\dot{u}_F - \dot{u}_S) = 0 \tag{11}$$

$$\eta^F \nabla p + \rho^F \ddot{u}_F + S_v(\dot{u}_F - \dot{u}_S) = 0 \tag{12}$$

$$T_E^S = 2u^S E_S + \lambda^S (E_S \cdot I)I \tag{13}$$

$$E_S = \frac{1}{2}(grad\, u_s + grad^T u_S), \tag{14}$$

where $u_i, \dot{u}_i, \ddot{u}_i, \rho^i; i = F, S$ are using for displacements, velocities, acceleration and density of fluid and solid parts respectively and p denote effective pore pressure of incompressible pore fluid. T_E^S Stands for stress and is the linearized Langrangian strain tensor in solid segment. λ^S and μ^S are the macroscopic Lame's parameters of porous solid and η^S and η^F are the volume fractions satisfying the relation

$$\eta^S + \eta^F = 1. \tag{15}$$

The tensor S_v relating the coupled interaction flanked by solid and fluid, in isotropic permeability may be define as

$$S_v = \frac{(\eta^F)^2 \gamma^{FR}}{K^F} I, \tag{16}$$

where γ^{FR} and K^F are fluid's specific weight and Darcy's permeability coefficient respectively.

The displacement vector $u_i (i = F, S)$ in two dimensional problems can be taken as

$$u_i = (u^i, 0, w^i) \text{ where } i = F, S. \tag{17}$$

Using equation (17) in equations (10) to (13) following equations are obtained as

$$(\lambda^S + \mu^S)\frac{\partial \theta^S}{\partial x} + \mu^S \nabla^2 u^S - \eta^S \frac{\partial p}{\partial x} - \rho^S \frac{\partial^2 u^S}{\partial t^2} + S_v\left[\frac{\partial u^F}{\partial t} - \frac{\partial u^S}{\partial t}\right] = 0 \tag{18}$$

$$(\lambda^S + \mu^S)\frac{\partial \theta^S}{\partial z} + \mu^S \nabla^2 w^S - \eta^S \frac{\partial p}{\partial z} - \rho^S \frac{\partial^2 w^S}{\partial t^2} + S_v\left[\frac{\partial w^F}{\partial t} - \frac{\partial w^S}{\partial t}\right] = 0 \tag{19}$$

$$\eta^F \frac{\partial p}{\partial x} + \rho^F \frac{\partial^2 u^F}{\partial t^2} + S_v\left[\frac{\partial u^F}{\partial t} - \frac{\partial u^S}{\partial t}\right] = 0 \tag{20}$$

$$\eta^F \frac{\partial p}{\partial z} + \rho^F \frac{\partial^2 w^F}{\partial t^2} + S_v\left[\frac{\partial w^F}{\partial t} - \frac{\partial w^S}{\partial t}\right] = 0 \tag{21}$$

$$\eta^S\left[\frac{\partial^2 u^S}{\partial x \partial t} + \frac{\partial^2 w^S}{\partial z \partial t}\right] + \eta^F\left[\frac{\partial^2 u^F}{\partial x \partial t} + \frac{\partial^2 w^F}{\partial z \partial t}\right] = 0. \tag{22}$$

Also, t_{zz}^s and t_{zx}^s are normal and tangential stresses in solid part respectively and written as in this way

$$t_{zz}^s = \lambda^S\left(\frac{\partial u^S}{\partial x} + \frac{\partial w^S}{\partial z}\right) + 2\mu^S \frac{\partial w^S}{\partial z} \tag{23}$$

$$t_{zx}^s = \mu^S\left(\frac{\partial u^S}{\partial z} + \frac{\partial w^S}{\partial x}\right), \tag{24}$$

where

$$\theta^S = \frac{\partial(u^S)}{\partial x} + \frac{\partial(w^S)}{\partial x} \tag{25}$$

and

$$\nabla^2 \equiv \frac{\partial^2}{\partial x^2} + \frac{\partial^2}{\partial z^2}. \tag{26}$$

In fluid and solid phase, displacement components (i.e. u^j and w^j) are associated to dimensional potential (i.e. ϕ^j and ψ^j) as

$$u^j = \frac{\partial \phi^j}{\partial x} + \frac{\partial \psi^j}{\partial z} \quad w^j = \frac{\partial \phi^j}{\partial z} - \frac{\partial \psi^j}{\partial x} \quad j = F, S. \tag{27}$$

Making use of equation (27), so the equations (10) to (13) can be written as

$$\nabla^2 \phi^S = \frac{1}{\overline{C}^2} \frac{\partial \phi^S}{\partial t^2} - \frac{S_v}{(\lambda^S + 2\mu^S)(\eta^F)^2} \frac{\partial \phi^S}{\partial t} = 0 \tag{28}$$

$$\phi^F = -\frac{\eta^S}{\eta^F} \phi^S \tag{29}$$

$$\mu^S \nabla^2 \psi^S - \rho^S \frac{\partial^2 \psi^S}{\partial t^2} + S_v \left[\frac{\partial \psi^F}{\partial t} - \frac{\partial \psi^S}{\partial t} \right] = 0 \tag{30}$$

$$\rho^F \frac{\partial \psi^F}{\partial t^2} + S_v \left[\frac{\partial \psi^F}{\partial t} - \frac{\partial \psi^S}{\partial t} \right] = 0 \tag{31}$$

$$(\eta^F)^2 p - \eta^S \rho^F \frac{\partial^2 \phi^S}{\partial t^2} - S_v \frac{\partial \phi^S}{\partial t} = 0, \tag{32}$$

where

$$\overline{C} = \sqrt{\frac{(\eta^F)^2 (\lambda^S + 2\mu^S)}{(\eta^F)^2 \rho^S + (\eta^S)^2 \rho^F}}. \tag{33}$$

Assuming the solution of the system of equations (28) to (32) in the form

$$(\phi^S, \phi^F, \psi^S, \psi^F, p) = (\phi_1^S, \phi_1^F, \psi_1^S, \psi_1^F, p_1) \exp(i\overline{\omega}t), \tag{34}$$

where $\overline{\omega}$ is the complex circular frequency.

Making the use of (34) in equations (28) to (32), obtained the results

$$\left[\nabla^2 + \frac{\overline{\omega}}{\overline{c}^2} - \frac{i\overline{\omega} S_v}{(\lambda^S + 2\mu^S)(\eta^F)^2} \right] \phi_1^S = 0 \tag{35}$$

$$[\mu^S \nabla^2 + \rho^S \overline{\omega}^2 - i\overline{\omega} S_v] \psi_1^S = -i\overline{\omega} S_v \psi_1^S = 0 \tag{36}$$

$$[-\overline{\omega}^2 \rho^F + i\overline{\omega} S_v] \psi_1^F - i\overline{\omega} S_v \psi_1^S = 0 \tag{37}$$

$$(\eta^F)^2 p_1 + \eta^S \rho^F \overline{\omega}^2 \phi_1^S - i\overline{\omega} S_v \phi_1^S = 0 \tag{38}$$

$$\phi_1^F = -\frac{\eta^S}{\eta^F} \phi_1^S. \tag{39}$$

Equation (35) corresponds to longitudinal wave propagating with velocity $\overline{V}_1$, given by

$$\overline{V}_1^2 = \frac{1}{G_1}$$

where

$$G_1 = \left[\frac{1}{\overline{C}^2} - \frac{iS_v}{\overline{\omega}(\lambda^S + 2\mu^S)(\eta^F)^2}\right]. \tag{41}$$

From equation (36) and (37) obtained the equation

$$\left[\nabla^2 + \frac{\overline{\omega}^2}{V_2^2}\right]\psi_1^S = 0. \tag{42}$$

Equation (42) corresponds to transverse wave propagating with velocity $\overline{V}_2$, given by $\overline{V}_2^2 = \frac{1}{G_2}$.

where

$$G_2 = \left\{\frac{\rho^S}{\mu^S} - \frac{iS_v}{\mu^S\overline{\omega}} - \frac{S_v^2}{\mu^S(-\rho^S\overline{\omega}^2 + i\overline{\omega}S_v)}\right\}. \tag{43}$$

3. Solution of Problem

The potential function for Medium M_1, can be written as:

$$q = B_0 \exp\{ik_0(x \sin\theta_0 - z\cos\theta_0) + i\omega_1 t\}$$
$$+B_1 \exp\{ik_0(x\sin\theta_1 + z\cos\theta_1) + i\omega_1 t\} \tag{44}$$

$$U_2 = B_2 \exp\{i\delta_1(x\sin\theta_2 + z\cos\theta_2) + i\omega_2 t\}$$
$$+B_3 \exp\{i\delta_2(x\sin\theta_3 + z\cos\theta_3) + i\omega_3 t\} \tag{45}$$

$$\phi_2 = EB_2 \exp\{i\delta_1(x\sin\theta_2 + z\cos\theta_2) + i\omega_2 t\}$$
$$+FB_3 \exp\{i\delta_2(x\sin\theta_3 + z\cos\theta_3) + i\omega_3 t\}, \tag{46}$$

where

$$E = \frac{\delta_1^2\,\omega_0^2}{c_4^2\delta_1^2 + 2\omega_0^2 - \omega_2^2 - \varepsilon^2\delta_1^2\dot{\omega}_2^2} \tag{47}$$

$$F = \frac{\delta_2^2\,\omega_0^2}{c_4^2\delta_2^2 + 2\omega_0^2 - \omega_3^2 - \varepsilon^2\delta_2^2\dot{\omega}_3^2}, \tag{48}$$

where B_0, B_1, B_2, B_3 are amplitudes of incident longitudinal wave, reflected longitudinal displacement, transverse and micro-rotation waves respectively.

For the medium M_2

The wave field due to incident, reflected and transmitted waves are given by

$$\{\phi^S, \phi^F, p\} = \{1, m_1, m_2\}\{\bar{A}_1 \exp\{i\bar{k}_1(x\sin\bar{k}_0 - z\cos\bar{k}_0) + i\bar{\omega}_1 t\} \quad (49)$$

$$\{\psi^S, \psi^F\} = \{1, m_3\}\{\bar{A}_2 \exp\{i\bar{k}_2(x\sin\bar{k}_0 - z\cos\bar{k}_0) + i\bar{\omega}_2 t\}, \quad (50)$$

where

$$m_1 = -\frac{\eta^S}{\eta^F} \quad m_2 = -\left[\frac{\eta^S\bar{\omega}_1^2\rho^F - i\bar{\omega}_1 S_v}{(\eta^F)^2}\right] \quad m_3 = \frac{i\bar{\omega}_2 S_v}{i\bar{\omega}_2 S_v - \bar{\omega}_2^2\rho^F}$$

$\bar{A}_1$ and $\bar{A}_2$ are amplitude of reflected P-wave as well as reflected SV-wave respectively. $\bar{k}_1$ and $\bar{k}_2$ represents the wave numbers of reflected P and SV-wave respectively.

4. Boundary Conditions for Welded Contact Interface

At the interface $z = 0$, between micropolar elastic solid with non-locality and fluid saturated porous solid is considered to be in perfect contact. The appropriate boundary conditions are continuity of force stresses, couple stress and displacements respectively. Mathematically, these boundary conditions can be written as:

At the interface $z = 0$,

$$(1-\varepsilon^2\nabla^2)\sigma_{kl} = t_{kl}^S - p\,(1-\varepsilon^2\nabla^2)\sigma_{kl} = t_{kl}^S\,(1-\varepsilon^2\nabla^2)m_{kl} = 0 \quad u_k = u^S. \quad (50)$$

For this model, these boundary conditions can be written from in the view of (1) and (2), so the first boundary condition is that the difference of normal stress components in z direction, of fluid and solid respectively equal to the fluid pressure p; second boundary condition is that tangential force per unit area are equal at this interface; third condition is that couple stresses is vanishes at this interface; due to continuity of displacement component and welded contact of the interface horizontal and vertical displacement are same. So, the suitable boundary conditions for the model under consideration, in mathematical form are taken as

$$\sigma_{zz} = t_{zz}^S - p \quad \sigma_{zx} = t_{zx}^S \quad m_{zy} = 0 \quad u_1 = u^s \; u_3 = w^s. \tag{52}$$

In order to gratify above said boundary conditions, the Snell's law's extension can be written as

$$\frac{\sin\theta_0}{V_0} = \frac{\sin\theta_1}{V_1} = \frac{\sin\theta_2}{V_3} = \frac{\sin\theta_3}{V_4} = \frac{\sin\bar{\theta}_1}{\bar{V}_1} = \frac{\sin\bar{\theta}_2}{\bar{V}_2}. \tag{53}$$

For the incident longitudinal wave

$$V_0 = V_1 \text{ and } \theta_0 = \theta_1.$$

Eventually, obtained a non-homogeneous system of five equations in matrix from

$$AZ = B \tag{54}$$

$$Z = [Z_1 \quad Z_2 \quad Z_3 \quad Z_4 \quad Z_5]^t \tag{55}$$

$$Z_1 = \frac{B_1}{B_0} \quad Z_2 = \frac{B_2}{B_0} \quad Z_3 = \frac{B_3}{B_0} \quad Z_4 = \frac{\bar{A}_1}{B_0} \quad Z_5 = \frac{\bar{A}_2}{B_0}. \tag{56}$$

where Z_1 to Z_5 are the amplitude ratios of reflected longitudinal displacement, reflected transverse and micro-rotational waves and refracted P and SV waves.

The elements of matrix are can be written as:

$$a_{11} = \{\lambda + (2\mu + \kappa)\cos^2\theta_1\} \quad a_{12} = (2\mu + \kappa)\sin\theta_3\cos\theta_3\frac{\delta_1^2}{k_1^2}$$

$$a_{13}(2\mu + \kappa)\sin\theta_4\cos\theta_4\frac{\delta_1^2}{k_1^2} \quad a_{14} = \frac{\bar{k}_1^2}{k_1^2}\{\lambda^S + 2\mu^S\cos^2\bar{\theta}_1 + m_2\}$$

$$a_{15} = -\frac{\bar{k}_2^2}{k_1^2}2\mu^S\sin\bar{\theta}_2\cos\bar{\theta}_2 \quad Y_1 = -a_{11}$$

$$a_{21} = -(2\mu + \kappa)\sin\theta_1\cos\theta_1$$

$$a_{22} = -\left\{\mu(\cos^2\theta_3 - \sin^2\theta_3) + \kappa\cos^2\theta_3 - \frac{\kappa E}{\delta_1^2}\right\}\frac{\delta_1^2}{k_1^2}$$

$$a_{23} = -\left\{\mu(\cos^2\theta_4 - \sin^2\theta_4) + \kappa\cos^2\theta_4 - \frac{\kappa F}{\delta_2^2}\right\}\frac{\delta_2^2}{k_1^2}$$

$$a_{24} = -2\mu^S \sin\bar{\theta}_1 \cos\bar{\theta}_1 \frac{\bar{k}_1^2}{k_1^2} \quad a_{25} = \mu^S(\cos^2\bar{\theta}_2 - \sin^2\bar{\theta}_2 \frac{\bar{k}_2^2}{k_1^2}$$

$$Y_1 = a_{21}$$

$$a_{31} = a_{34} = a_{35} = Y_3 = 0 \quad a_{32} = -E \quad a_{33} = -F$$

$$a_{41} = \sin\theta_1 \quad a_{42} = \cos\theta_3 \frac{\delta_1}{k_1}$$

$$a_{43} = \cos\theta_4 \frac{\delta_2}{k_1} \quad a_{44} = -\sin\bar{\theta}_1 \frac{\bar{k}_1}{k_1}$$

$$a_{45} = -\sin\bar{\theta}_2 \frac{\bar{k}_2}{k_1} \quad Y_4 = -a_{41}$$

$$a_{51} = \cos\theta_1 \quad a_{52} = -\sin\theta_3 \frac{\delta_1}{k_1}$$

$$a_{53} = -\sin\theta_4 \frac{\delta_2}{k_1} \quad a_{54} = -\cos\bar{\theta}_1 \frac{\bar{k}_1}{k_1}$$

$$a_{55} = -\sin\bar{\theta}_2 \frac{\bar{k}_2}{k_1} \quad Y_5 = -a_{51}. \tag{57}$$

5. Numerical Results and Discussion

System of five non-homogeneous equations obtained the various amplitude ratios of reflected and refracted waves for emergence longitudinal wave. In order to understand the behavior of different amplitude ratios, in detail, these ratios are computed numerically for the considered model by taking the values of applicable elastic parameters.

Consider the medium M_1 as silicon crystal, so the physical constants are

$$\lambda = 0.1055 \times 10^{12}\mathrm{N/m^2} \quad \mu = 0.2518 \times 10^{11}\mathrm{N/m^2}$$

$$\kappa = 0.1 \times 10^{11} N/m^2 \quad e_0 = 0.49$$

$$j = 9.21 \times 10^{-16} \mathrm{m}^2 \quad \rho = 2330 \mathrm{kg/m}^3$$

$$\gamma = 8695.99 \times 10^{-8} \mathrm{N} \ a = 0.5431 \times 10^{-9} \mathrm{N}. \tag{58}$$

In the second medium M_2, the values of various parameters are

$$\eta^S = 0.67 \quad \eta^F = 0.33$$

$$\rho^S = 1.34 \mathrm{Mg/m}^3 \quad \lambda^S = 5.5833 \mathrm{MN/m}^2$$

$$K^F = 0.01 \mathrm{m/s} \quad \mu^S = 8.3750 \mathrm{N/m}^2$$

$$\gamma^{FR} = 10.00 \mathrm{KN/m}^3 \quad \rho^F = 0.33 \mathrm{Mg/m}^3$$

$$\overline{\omega} = 10/\mathrm{s}. \tag{59}$$

Determines the modulus of amplitude ratios of different reflected and refracted waves for this particular model and MATLAB software (R2015a 32-bit) has been used for numerical computation of the resulting non-dimensional coefficients and illustrate these ratios graphically. The amplitude ratios are computed for incidence angle changes from $\theta = 0^\circ$ to $\theta = 90^\circ$. The disparity of modulus of amplitude ratios i.e. $| Z_i | (i = 1, 2, 3, 4$ and 5) with emergence angle θ_0 of longitudinal wave are revealed in figures.

In figures (2) and (3), describes the variations of amplitude ratios when the incident wave is longitudinal wave when medium M_1 is micropolar elastic solid with non-locality and medium M_2 is fluid saturated porous solid. This case is represented by 'General' and uses its abbreviation "GEN" in the figures. The tendency of dependence of $| Z_i |$ on incident wave as well as angle of incidence is dissimilar for different reflected and refracted waves as depicted in the figures.

In the figure (2) represent the dissimilarities of the values of the amplitude ratios $| Z_1 |, | Z_2 |$ and $| Z_3 |$ from the angle of emergence $\theta_0 = 0^\circ$ to $\theta_0 = 90^\circ$. Here the values of the amplitude ratios $| Z_2 |$ and $| Z_3 |$ are vanishes zero at $\theta_0 = 0^\circ$ and $\theta_0 = 90^\circ$ while the value of amplitude ratio

$|Z_1|$ is non-zero at the same angle. The amplitude ratios $|Z_1|$ and $|Z_3|$ have common value at angle $\theta_0 = 28^\circ$ and $\theta_0 = 74^\circ$ whereas the ratios $|Z_1|$ and $|Z_2|$ have point of intersection common value at angle $\theta_0 = 58^\circ$ and $\theta_0 = 66^\circ$. Except such angles, all amplitude ratios have totally different values from $\theta_0 = 0^\circ$ to $\theta_0 = 90^\circ$. The values of $|Z_1|$ are very smoothly increases from initial angle to $\theta_0 = 58^\circ$ and then the values rapidly decreases from the angle $\theta_0 = 58^\circ$ to $\theta_0 = 64^\circ$ and approaches to its local minima and after that the values again increase according to angle of emergence. The values of $|Z_2|$ are smoothly increases from the initial angle i.e. $\theta_0 = 0^\circ$ to $\theta_0 = 60^\circ$ and obtain its peak value and then values suddenly decreases up-to $\theta_0 = 65^\circ$ and after all the values again smoothly decreases corresponds to angle of emergence. Now, the values of $|Z_3|$ are smoothly increases from the initial angle i.e. $\theta_0 = 0^\circ$ to $\theta_0 = 60^\circ$ and obtain its peak value and then values suddenly decreases up-to $\theta_0 = 65^\circ$ and finally the values again smoothly decreases corresponds to angle of emergence. In this figure, all the values of $|Z_3|$ are greater than the values of $|Z_2|$ apart from only two angle i.e. $\theta_0 = 0^\circ$ and $\theta_0 = 90^\circ$ whereas the values of $|Z_3|$ are lesser from the angle $\theta_0 = 0^\circ$ to $\theta_0 = 27^\circ$ and $\theta_0 = 74^\circ$ to $\theta_0 = 90^\circ$ as compare to the values of $|Z_1|$. The values of $|Z_1|$ are smaller than the values of $|Z_3|$ from $\theta_0 = 27^\circ$ to $\theta_0 = 90^\circ$. The effects of the non-locality are very clearly visible in the above figure.

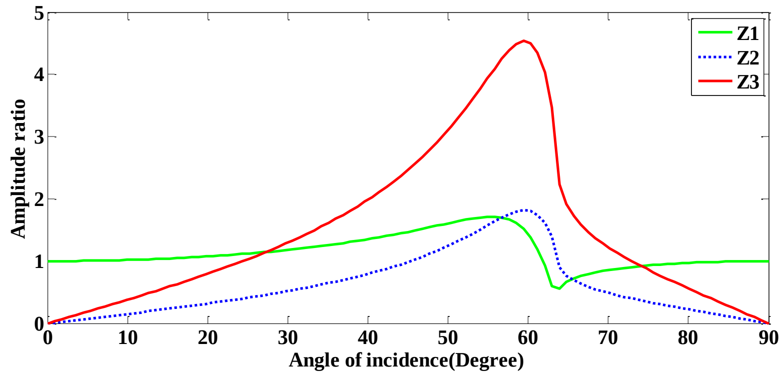

The figure (3) describes the variation of the values of $|Z_4|$ and $|Z_5|$ from the angle of emergence $\theta_0 = 0^\circ$ to $\theta_0 = 90^\circ$. Here the value of the ratios $|Z_4|$ and $|Z_5|$ are obtains zero at $\theta_0 = 0^\circ$ and $\theta_0 = 90^\circ$. The ratios $|Z_4|$ and $|Z_5|$ have point of intersection common value at angle $\theta_0 = 29^\circ$. Except the angles $\theta_0 = 0^\circ$, $\theta_0 = 29^\circ$, and $\theta_0 = 90^\circ$, both of amplitude ratios have totally different values from the initial angle to last angle. The values of $|Z_4|$ are very smoothly increases from initial angle to $\theta_0 = 60^\circ$ and then the values rapidly decreases from the angle $\theta_0 = 60^\circ$ to $\theta_0 = 65^\circ$ and after that the values again smoothly decreases according to angle of emergence and again attains its local minima. The values of $|Z_5|$ are increases very slowly from $\theta_0 = 0^\circ$ to $\theta_0 = 60^\circ$ and then the values rapidly decreases from the angle $\theta_0 = 60^\circ$ to $\theta_0 = 65^\circ$ and after that the values again smoothly decreases according to angle of incidence. The values of $|Z_4|$ are smaller in comparison to the values of $|Z_5|$ from $\theta_0 = 0^\circ$ to $\theta_0 = 29^\circ$ except only the angle $\theta_0 = 0^\circ$ whereas values are greater from $\theta_0 = 29^\circ$ to $\theta_0 = 90^\circ$ except only $\theta_0 = 90^\circ$. It is concluding that under the consideration of the medium and boundary conditions the effect of non-locality is clearly seen in this figure.

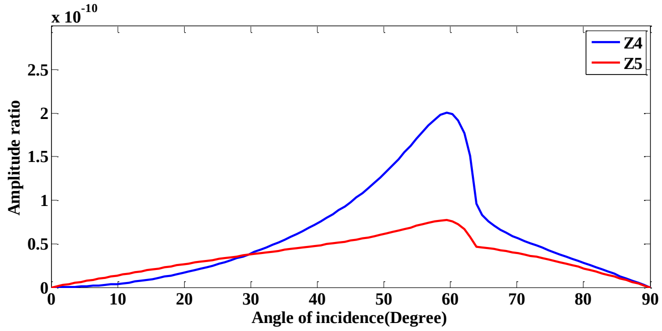

6. Conclusion

The tendency of reflection and refraction of emergent plane wave at an interface of non-local micropolar elastic solid and fluid saturated porous solid has investigated. Amplitude ratios of various reflected and refracted waves have been computed numerically for a specific model and thus the results are represented graphically with an angle of incidence of incident wave. Graphical behavior of amplitudes ratios of different waves are depicted by computing in MATLAB software and constant value of physical parameters and corresponding boundary conditions.

- Amplitude ratios of different waves depend on the emergence angle of emergent wave at the interface.

- The tendency of amplitudes ratios of various waves depend on angle θ_0 and properties of materials half spaces.

- Effects of non-locality are clearly visible in the figures.

References

[1] A. C. Eringen, Nonlocal polar elastic continua, International Journal of Engineering Science 10 (1972), 1-16.

[2] A. C. Eringen, Linear theory of nonlocal elasticity and dispersion of plane waves, International Journal of Engineering Science 10 (1972), 425-435.

[3] A. C. Eringen, Nonlocal Continuum Field Theories, Springer-Verlag, New York, 2002.

[4] A. C. Eringen and D. G. B. Edelen, On nonlocal elasticity, International Journal of Engineering Science 10 (1972), 233-248.

[5] A. C. Eringen, Plane waves in nonlocal micropolar elasticity, International Journal of Engineering Science 22 (1984), 1113-1121.

[6] J. Wang and R. S. Dhaliwal, On some theorems in the nonlocal theory of micro polar elasticity, International Journal of Engineering Science 1 (2006), 325-337.

[7] A. C. Eringen and E. S. Suhubi, Nonlinear theory of simple micro-elastic solids *I*, International Journal of Engineering Science 2 (1964), 189-203.

[8] A. C. Eringen, Micropolar elastic solids with stretch, Ari. Kitabevi Matabaasi 24:1-9.

[9] A. C. Eringen, Theory of micropolar elasticity, fracture (New York: Academic Press) vol. 2, 1968.

[10] A. Khurana and S. K. Tomar, Waves at interface of dissimilar nonlocal micro polar elastic half-spaces, Mechanics of Advanced Materials and Structures, vol. 0, 1-9, 2018.

[11] M. Gade and S. T. G. Raghukanth, Seismic ground motion in micropolar elastic half-space, Applied Mathematical Modeling 39 (2015), 7244-7265.

[12] N. Kumari, Wave propagation at micropolar elastic/fluid saturated porous solid interface, International Journal of Mathematical Archive 4(8) (2013), 56-66.

[13] P. Zhang, P. Wei and Y. Li, Reflection of longitudinal displacement wave at the viscoelastically supported boundary of micropolar half-space, Meccanica, 52:1641. doi:10.1007/S11012-016-0514-z, 2016.

[14] R. Kumar, M. L. Gogna and L. Debnath, On Lamb's problem in a micropolar viscoelastic half-space with stretch, International Journal of Mathematical Science 13 (1990), 363-327.

[15] R. D. Gautheir, Experimental investigations on micropolar media, Mechanics of Micropolar Media (eds.) O Brulin, R K T Hsieh (World Scientific, Singapore), p.395, 1982.

[16] R. De Boer, W. Ehlers and Z. Liu, One-dimensional transient wave propagation in fluid-saturated incompressible porous media, Archive of Applied Mechanics 63(1) (1993), 59-72.

[17] R. De. Boer, Theory of Porous Media, Springer, Berlin, 2000.

[18] S. K. Tomar and M. L. Gogna, Reflection and refraction of longitudinal microrotational wave at an interface between two different micropolar elastic solids in welded contact, International Journal of Engineering Science 30 (1992), 1637-1646.

[19] V. R. Parfitt and A. C. Eringen, Reflection of plane waves from the flat boundary of a micropolar elastic half space, J. Acoust. Soc. Am. 45 (1969), 1258-1272.

[20] W. Nowacki, The Linear Theory of Micropolar Elasticity, International Centre For Mechanical Sciences, Springer, New York, 1974.